

Antiferromagnetic topological insulators in cold atomic gases

Andrew M. Essin and Victor Gurarie

Department of Physics, CB390, University of Colorado, Boulder, Colorado 80309, USA

(Received 25 January 2012; published 10 May 2012)

We propose a spin-dependent optical lattice potential that realizes a three-dimensional antiferromagnetic topological insulator in a gas of cold, two-state fermions such as alkaline earths, as well as a model that describes the tight-binding limit of this potential. We discuss the physically observable responses of the gas that can verify the presence of this phase, in particular rapid rotation in response to the trap potential. We also point out how this model can be used to obtain two-dimensional flat bands with nonzero Chern number.

DOI: [10.1103/PhysRevB.85.195116](https://doi.org/10.1103/PhysRevB.85.195116)

PACS number(s): 67.85.-d, 03.65.Vf, 73.20.At, 75.50.Ee

I. INTRODUCTION

The use of cold atomic gases to implement many-body models of condensed matter physics is by now well advanced. The goal of this research is twofold: to simulate existing materials with cold atoms and to manufacture Hamiltonians unseen in solids.

A particularly strong effort in the field over the last decade has been directed toward recreating the integer and fractional quantum Hall effects with cold atoms by simulating an orbital magnetic field for neutral atoms, achieving slow but steady progress. The quantum Hall effects realize a large variety of topological states of matter. Not all of them have been unambiguously seen in semiconductor heterostructures, and some of those not yet obtained may be important for applications.¹ One hopes that quantum Hall effects with cold atoms will provide ways to investigate those states experimentally.

Parallel to that effort, a number of breakthroughs in condensed matter physics in recent years have led to an understanding that the integer quantum Hall effect is but one particular system in a class of noninteracting fermionic systems, in a variety of spatial dimensions, which have received the name of topological insulators (TIs).² All TIs have gapped bulk and gapless edge states, and respond to external electromagnetic perturbations in a quantized way.^{3,4} The quantum Hall effect is confined to two dimensions, but three-dimensional (3D) topological insulators have also been observed experimentally. In each spatial dimensionality there are five distinct types of topological insulators and superconductors,⁴ with only two of those five seen experimentally in three dimensions in real materials. Cold atoms may end up providing the only way to manufacture the 3D TIs not yet seen.

It is also suspected that in the presence of interactions TIs may develop phases similar in some sense to those of the fractional quantum Hall effect.⁵ Theoretical study of these interacting phases is currently a rapidly developing subject. While it is not yet known if these phases can be seen in a condensed matter context, it is natural to consider TIs with cold atoms, whose interactions can often be controlled or chosen in advance.

The distinctive signature of 3D TIs, in addition to gapless, Dirac-type excitations localized at the surfaces of the system, is a strong, quantized magnetoelectric response. The former is best seen as the 3D counterpart to the chiral edge states of the

integer quantum Hall phase, and the latter as the counterpart of the Hall conductance of that phase.

We propose a model that realizes an unusual (and thus far unseen) 3D TI, called the antiferromagnetic topological insulator (AFTI). The AFTI bulk is similar to the standard strong TI described by Refs. 6–8. However, time-reversal invariance, crucial to that type of a TI, is implemented in a different way, with the result that the magnetoelectric response of the TI becomes a ground-state property in the trap potential always present in cold atomic setups. As a result, in response to the applied trap potential this system starts rotating rapidly, a tell-tale signature that we hope can be used to detect this phase.

The model we propose can be implemented in cold atoms by an extension of the idea of artificial gauge fields.⁹ The construction involves atoms with only two internal states, and we hope not only that the model proposed here possesses features (magnetoelectric response to an applied scalar potential) making it more suitable for observation and study with cold atoms, but also that this provides a simplification compared to existing schemes to implement strong TIs,^{10,11} as we elaborate below.

Moreover, a tight-binding limit of this model acquires sublattice symmetry and is a chiral 3D TI.¹² This is a type of 3D insulator distinct from the standard strong TI and, like the AFTI, not yet seen experimentally in solids.

Finally, we propose to use this insulator as a way to create two-dimensional flat bands (surface bands of this insulator) with nonzero Chern number, which are known to have the potential to enhance interaction effects and therefore aid the formation of fractional quantum Hall states without strong magnetic fields.

II. ANTIFERROMAGNETIC TOPOLOGICAL INSULATORS

A starting point toward constructing a strong TI is an identification of a time-reversal operation \mathcal{T} that satisfies $\mathcal{T}^2 = -1$. If it is a symmetry, it ensures that the energy eigenstates come in degenerate Kramers pairs, which provides the simplest way to understand that the edge spectrum must be gapless.

Realization of the TI requires a minimum of four distinct states per wave vector \mathbf{k} . First, there needs to be some degree of freedom on which the symmetry \mathcal{T} can be realized, which requires two states that we call spin. With just these two states,

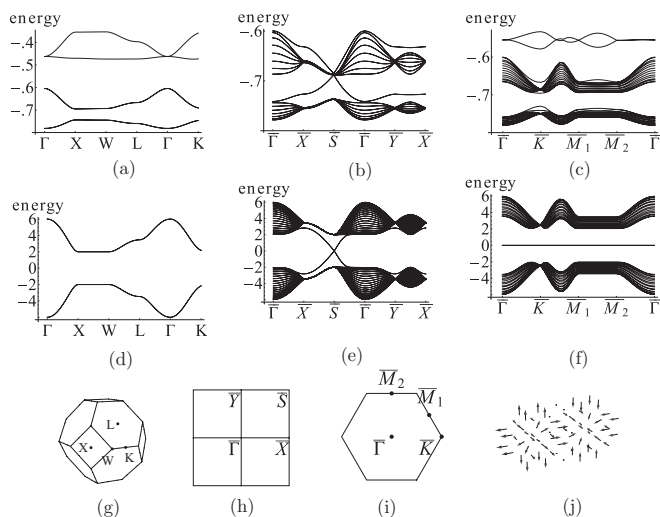


FIG. 1. The spectra of Eq. (1) in (a) bulk, (b) a (100) slab, and (c) a (111) slab, with parameters $B_Z = 3V/2 = \hbar^2 q^2/2m = 1$; and corresponding geometries for Eq. (2) [(d), (e), (f)] with parameters $t = t_M = 1$. (g) The bulk Brillouin zone; the zone center Γ is not shown. (h), (i) The (100) and (111) surface Brillouin zones. (j) $\mathbf{B}_Z(\mathbf{r})$.

however, there will not be a gap in the bulk band structure, so to achieve a band insulator there must be more states. The minimal implementations considered so far require four spin states, as in the proposal of Ref. 11.

In an effort to minimize the number of internal states that need to be manipulated, we propose instead to use two sublattices, limiting the number of internal (spin) states to two. Furthermore, we want to find a model on the simplest lattice possible, so we restrict to nearest-neighbor hopping terms; this rules out the diamond-lattice tight-binding model of Ref. 6, for example.

The simplest approach to achieve the physics of the TI that we have found realizes the AFTI.¹³ The prototype of such a system involves electrons that have a Zeeman coupling to an Néel order parameter. This obviously breaks \mathcal{T} because the order parameter flips under the action of time reversal, but the magnetic order may be such that the symmetry is restored after an appropriate translation. We represent this translation by a unitary operator $T_{1/2}$, for translation through half the magnetic unit cell; the symmetry is implemented by the antiunitary operator $S = \mathcal{T}T_{1/2}$, which satisfies $S^2 = -1$ and therefore has the crucial property necessary for nontrivial topological physics.

An AFTI has two distinct types of surface, called antiferromagnetic and ferromagnetic in this context. The first type preserves the symmetry S of the bulk, and therefore supports gapless surface states of Dirac type just like a surface of the usual TI. Ferromagnetic surfaces break the symmetry, which opens a gap, and the surface realizes a half-quantum-Hall effect, just like a surface of the usual TI with an added \mathcal{T} -breaking perturbation.^{3,14}

We have found a spin-dependent, optical lattice potential that realizes the AFTI, as well as a tight-binding model for the deep-well limit of this potential. The tight-binding model has an extra chiral symmetry which is interesting in its own right,⁴ and we display band structures in Fig. 1 both in the

chiral, tight-binding limit and far from it so generic features are distinguishable.

A. Optical lattice

The following spin-dependent, noninteracting Hamiltonian realizes an AFTI

$$H_{\text{AF}}(\mathbf{p}, \mathbf{r}, \mathbf{s}) = \frac{p^2}{2m} + V(\mathbf{r}) + \mathbf{B}_Z(\mathbf{r}) \cdot \boldsymbol{\sigma},$$

$$V(\mathbf{r}) = V [\cos q\hat{x} \cdot \mathbf{r} + \cos q\hat{y} \cdot \mathbf{r} + \cos q\hat{z} \cdot \mathbf{r}] \quad (1)$$

$$\mathbf{B}_Z(\mathbf{r}) = B_Z \sum_{i=1}^4 \mathbf{b}^i \cos(q\mathbf{b}^i \cdot \mathbf{r}),$$

where $q = 2\pi/a$ sets the length scale. Here \mathbf{p} and \mathbf{r} are the single-particle momentum and position; \hat{x} , \hat{y} , and \hat{z} are orthogonal unit vectors; and $\boldsymbol{\sigma}$ represents the vector of Pauli matrices. Finally, the tetrahedral vectors \mathbf{b}^i are defined as $\mathbf{b}^1 = (-\hat{x} + \hat{y} + \hat{z})/2$, $\mathbf{b}^2 = (\hat{x} - \hat{y} + \hat{z})/2$, $\mathbf{b}^3 = (\hat{x} + \hat{y} - \hat{z})/2$, $\mathbf{b}^4 = -(\hat{x} + \hat{y} + \hat{z})/2$.

The potential V creates a spin-independent, cubic lattice, while the Zeeman field $\mathbf{B}_Z(\mathbf{r})$, a sum of four one-dimensional, spin-dependent terms, creates an alternating magnetic hedgehog texture around the wells of that lattice [see Fig. 1(j)]. This is the NaCl structure, which has the translation symmetry of a face-centered-cubic (fcc) lattice.

The Zeeman field $\mathbf{B}_Z(\mathbf{r})$ breaks \mathcal{T} since $\boldsymbol{\sigma} = -\sigma_y \boldsymbol{\sigma}^* \sigma_y$, but the symmetry is restored by a translation $T_{1/2}$ through a (along any of the cubic axes). This Hamiltonian therefore has the symmetry S described earlier, which enables a topologically nontrivial phase.

This Hamiltonian is gapped at a filling of one particle for every well of $V(\mathbf{r})$, which is two particles per unit cell of \mathbf{B}_Z [see Fig. 1(a)]. (Each band is doubly degenerate since the combination of S and inversion is a symmetry; see below for inversion symmetry.) In other words, \mathbf{B}_Z gaps the simple cubic metal described by $p^2/2m + V$. The resulting insulator is topologically nontrivial, which is computed most simply as follows. In addition to the symmetry S , this Hamiltonian also possesses inversion symmetry $(\mathbf{p}, \mathbf{r}) \rightarrow -(\mathbf{p}, \mathbf{r})$. This allows us to compute the bulk topological invariant [Eq. (6) of Ref. 15] in terms of inversion parities at the eight inversion-symmetric wave vectors $\Gamma = 0$, $(\mathbf{X}^1, \mathbf{X}^2, \mathbf{X}^3) = \pi(\hat{x}, \hat{y}, \hat{z})$, and $\mathbf{L}^i = \pi \mathbf{b}^i$. We find that at Γ both filled bands are inversion even, at \mathbf{X}^i both are inversion odd, and at \mathbf{L}^i there are one of each parity. The total number of inversion-odd states is 10, which is twice an odd number; therefore the band structure is topologically nontrivial. (Note that the prescription of Ref. 16 does not apply to this system since the Kramers pairs are not degenerate with respect to inversion at \mathbf{L}^i .)

In this potential, a surface normal to \hat{x} , \hat{y} , or \hat{z} [a (100)-type surface] retains the symmetry S of the bulk, and so is an antiferromagnetic surface in the terminology of Ref. 13. Such a surface possesses gapless edge states, as seen in Fig. 1(b). By contrast, a surface normal to \mathbf{b}^i [a (111)-type surface] breaks the symmetry and is gapped, as in Fig. 1(c). These surfaces support a half-quantum-Hall effect.

B. Tight-binding model

In the deep-well limit, the Hamiltonian (1) reduces to the following tight-binding model on the cubic lattice with nearest-neighbor, spin-dependent hopping terms (both t and t_M are real)

$$\begin{aligned}\hat{H}_{\text{tb}} &= \sum_{\mathbf{r} \in A} \sum_{\mathbf{e}} \hat{c}_{\mathbf{r}}^\dagger [t + t_M \mathbf{e} \cdot \boldsymbol{\sigma}] \hat{c}_{\mathbf{r}+\mathbf{e}} + \text{H.c.} \\ &= \sum_{\mathbf{r}, \mathbf{r}'} \hat{c}_{\mathbf{r}}^\dagger \mathcal{H}_{\mathbf{r}, \mathbf{r}'} \hat{c}_{\mathbf{r}'}.\end{aligned}\quad (2)$$

Here $\hat{c}_{\mathbf{r}}$ removes an atom at site \mathbf{r} , $\mathbf{e} \in \{\pm \hat{x}, \pm \hat{y}, \pm \hat{z}\}$, \mathcal{H} is the matrix of \hat{H}_{tb} , and the spin indices have been suppressed on \hat{c} , $\boldsymbol{\sigma}$, and \mathcal{H} ; A signifies one of the two sublattices of the bipartite division of the cubic lattice. This model captures the hedgehog character of Zeeman field \mathbf{B}_Z . Starting from sublattice A , the barrier to tunneling in the $+\hat{z}$ direction is higher for an atom with $\sigma^z = +1$ than for one with $\sigma^z = -1$, and the barriers to tunneling along $-\hat{z}$ are interchanged. These statements also hold for $z \rightarrow x, y$.

The bulk spectrum is given by

$$\begin{aligned}\mathcal{H}_{\mathbf{k}} &= 2 \begin{pmatrix} 0 & g_{\mathbf{k}} \\ g_{\mathbf{k}}^\dagger & 0 \end{pmatrix}, \quad \epsilon(\mathbf{k}) = \pm 2 \sqrt{t^2 f_{\mathbf{k}}^2 + t_M^2 f_{M\mathbf{k}}}, \\ g_{\mathbf{k}} &= \sum_{j \in \{x, y, z\}} (t \cos k_j - it_M \sigma^j \sin k_j), \\ f_{\mathbf{k}} &= \sum_{j \in \{x, y, z\}} \cos k_j, \quad f_{M\mathbf{k}} = \sum_{j \in \{x, y, z\}} \sin^2 k_j,\end{aligned}\quad (3)$$

and shown in Fig. 2(d), where $\mathcal{H}_{\mathbf{k}}$ is the Fourier transform of $\mathcal{H}_{\mathbf{r}, \mathbf{r}'}$ and is a matrix in sublattice as well as spin space. As expected, it resembles the lowest two (doubly degenerate) bands of the optical lattice model in Fig. 1(a), particularly in that each band is doubly degenerate at each wave vector. Note that there is a gap whenever $t, t_M \neq 0$. In the deep-well limit, the higher bands of Fig. 1(a) move off to high energies.

The tight-binding model has more symmetry than does H_{AF} : $\Sigma \mathcal{H} \Sigma^{-1} = -\mathcal{H}$, where $\Sigma_C A = c_A$, $\Sigma_C B = -c_B$ on sublattices A and B . This is known as sublattice or chiral symmetry,^{4,17} which places this model into symmetry class DIII, akin to phase B of ^3He .¹⁸ The associated topological invariant is particularly straightforward to evaluate^{4,19,20}

$$\begin{aligned}N_3 &= \pi \int \frac{d^3 k}{(2\pi)^3} \frac{1}{3!} \epsilon_{abc} \text{tr} \Sigma D^a D^b D^c = 1, \\ D^a &= \mathcal{H}_{\mathbf{k}}^{-1} \partial_{k_a} \mathcal{H}_{\mathbf{k}},\end{aligned}\quad (4)$$

where the integral is over the fcc Brillouin zone.

The surface bands of \hat{H}_{tb} are shown in Figs. 1(e) and 1(f). They, too, resemble the corresponding spectra for the optical lattice potential. On the (100) surface the Dirac point sits in the center of the gap. More remarkably, on the (111) surface the disconnected bands that can be seen above the upper band in Fig. 1(c) also migrate to the center of the gap in the tight-binding limit. That band, once at zero energy, is protected by chiral symmetry (in this geometry there is only chiral symmetry, so the system is formally in class AIII) and is necessarily flat (the states in that band occupy one of the two sublattices

and their energy is protected by the index theorem as explained, for example, in Ref. 21, or by a theorem of Lieb).²² Moreover, it can be checked numerically that this flat band has Chern number 1; this is like the zeroth Landau level of a Dirac mode.²³

III. MAGNETOELECTRIC RESPONSE IN ULTRACOLD ATOMIC GASES

There has recently been much discussion of topologically nontrivial flat bands as a way to realize fractional quantum Hall physics without an external magnetic field; typical cases require tuning of parameters to achieve a very flat band.²⁴ Here the flatness is perfect when the surfaces respect the sublattice symmetry, with no tuning.

To realize the Hamiltonian Eq. (1) or its tight binding version Eq. (2) we need to employ atoms with two internal levels, representing spin, which can be coupled by a laser. A particularly promising approach would be to use for these two levels the ground (3S_0) and excited (3P_0) states of fermionic alkaline-earth-like atoms such as Sr or Yb; this is attractive due to the extremely long lifetime of the excited state and the fact that these states can be coupled directly by an optical laser.

The tight-binding Hamiltonian Eq. (2) may be created by directly imprinting the tunneling matrices onto the atoms following Ref. 25. Alternatively, let us describe realizing the potential of Eq. (1). Working with the alkaline-earth-like atoms, the scalar potential and σ_z can be realized with lasers at magic and antimagic wavelengths,²⁵ while σ_x and σ_y potentials require a laser operating at the 1S_0 - 3P_0 transition frequency. Matching the wavelengths of these lasers would require setting up two traveling waves at an angle for every standing wave potential. Note that the 3P_0 state is known to be collisionally unstable. We can eliminate this instability if we polarize the nuclear spins of the atoms preventing two 3P_0 atoms from scattering in the s -wave channel. 3P_0 - 1S_0 collisions may also be unstable, although recent experiments indicate that at least in ^{87}Sr this instability is weak (below experimental sensitivity).²⁶

Let us now turn to discussing how to see the physics of this TI in an optical lattice. In a crystal, the most dramatic consequence is the presence of the surface states displayed above. The topological surface states have a Dirac-like spectrum that connects the bulk bands. While there is some spectroscopic information available for atomic gases,²⁷ a more productive approach may be to look at macroscopic properties, in particular the response of the gas to external forces.

Consider atoms of mass m subject to an additional, constant external force \mathbf{F} . The orbital response tensor is $\alpha_j^i = \partial \mathcal{L}_j / \partial F_i$, where \mathcal{L} is the average angular momentum density. One expects this quantity to vanish in linear response when the potential possesses time-reversal and/or inversion symmetry. However, in a TI with surface \mathcal{T} breaking, it takes the surprisingly large, isotropic value

$$\alpha_j^i = \pm \frac{m}{h} \delta_j^i, \quad (5)$$

where h is Planck's constant.²⁸ This response is very strong. Indeed, applying a force of the order of E_r/d , where d is

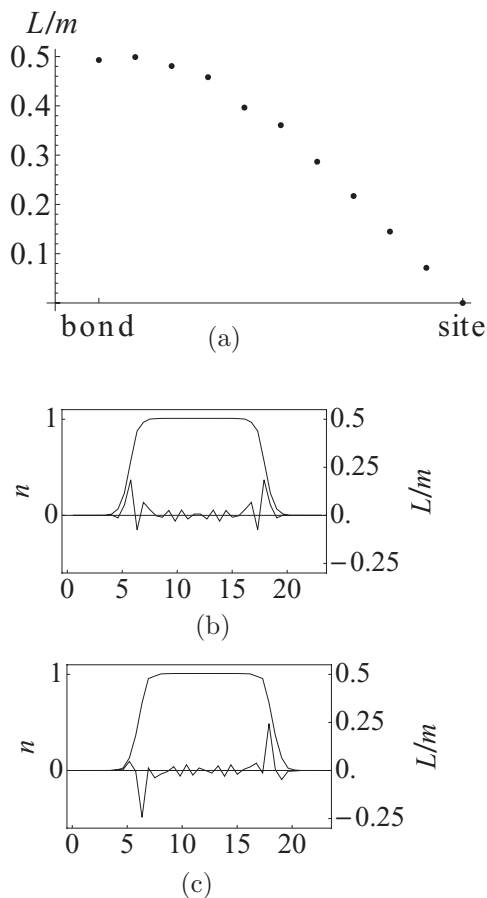


FIG. 2. (a) Net circulation L/m per two-dimensional unit cell in a harmonic trap, in units of ta^2/h , for $t_M = t$, $m\omega^2 a^2 = t/4$, $\mu = 1.5t$. The abscissa gives the position of the trap center relative to the lattice. Also shown are the circulation L/m (lower curve) and particle number per site n (upper) as a function of position (in units of a) for (b) a bond-aligned and (c) a site-aligned trap.

the linear size of the system and $E_r = h^2/(ma^2)$ is the lattice recoil energy, we find from Eq. (5) that the induced angular momentum is of the order $h(d/a)^2$, that is one quantum per 2D unit cell. That far exceeds what was achieved by rotating the atomic gases directly,²⁹ recent progress in this effort notwithstanding.³⁰

The striking signature of the TI phase in a gas of fermions should then be a rotation of the cloud in response to a linear potential gradient, if there were some \mathcal{T} breaking present. In the present case, a parabolic trap will necessarily break all the relevant symmetries (both chiral symmetry if present and S , since it involves translations), enabling a strong response.

In fact, the mere presence of the trap induces rotation in general; after all, shifting the trap by Δs is essentially equivalent to a force $m\omega^2 \Delta s$, for trap frequency ω . We have computed the circulation for a gas tightly confined in the [111] direction by a harmonic trap (see Fig. 2). To make this numerically tractable we have imposed periodic boundary conditions (we do not expect a weak, parabolic 2D trap to change any resulting physics), and computed the circulation

per 2D unit cell for \hat{H}_{tb} ,³¹

$$\frac{L}{mN_s a^2} = \frac{\pi}{i\hbar} \int \frac{d^2 k}{(2\pi)^2} \epsilon_{ab} \text{tr} (P - Q)(\partial^a P) \tilde{\mathcal{H}}(\partial^b P), \quad (6)$$

on a 100-by-100 grid of the (111) Brillouin zone. Here $\tilde{\mathcal{H}}$ is the two-dimensional Fourier transform of $\mathcal{H}_{\mathbf{r},\mathbf{r}'} + m\omega^2 s^2/2 - Fs - \mu$, with s the [111] coordinate; P (Q) projects onto the negative- (positive-)energy states of $\tilde{\mathcal{H}}$; and N_s is the number of surface unit cells. The sign of L changes for alternate bonds, since the \mathcal{T} -breaking term switches sign. The derivative $|\partial(L/Na^3)/\partial F| \lesssim 0.5m/h$, in agreement with Eq. (5), when the trap is aligned with lattice sites; here N is the particle number, and provides a suitable measure of the size of the trapped system since the bulk density is one particle per site. The rotation takes its maximum when the trap is aligned with the bond centers, and the circulation is concentrated mainly at the surfaces, as is clear from Figs. 2(b) and 2(c).

The resulting rotation may be measured with a variety of methods: for example, by switching off the lattice and observing a flattening of the rotating cloud; by measuring the way the Fourier-transformed density distribution $n_{\mathbf{k}}$ vanishes at $\mathbf{k} = 0$; by measuring the frequency modes of the rotating gas;³² or by Bragg spectroscopy.³³

Note that the response tensor α is well defined even in the presence of interactions. The invariant for the chiral limit is similarly well defined with interactions, using Green's function rather than the single-particle Hamiltonian.³⁴ That is, the TI phase should be stable to the introduction of weak interactions. It would be interesting to check this result directly in cold Fermi gases, which display Feshbach resonances that lead to tunable interactions (although that might require using alkali atoms coupled by Raman transitions instead of alkaline earths as outlined above); it would be even more interesting to study the Mott-type phases that should emerge upon introducing very strong interactions.³⁵

Finally, it is worth pointing out connections to other systems that display interesting behavior in the presence of magnetic textures. In particular, such textures have been argued to be give an important contribution to the anomalous Hall effect in colossal magnetoresistance materials³⁶ and in MnSi.³⁷ Such textures can be produced with a Zeeman field, such as of Eq. (1), when it is incommensurate with the lattice or when the lattice is absent entirely.

ACKNOWLEDGMENTS

We thank E. A. Cornell, C. Vale, P. Drummond, M. D. Swallows, and especially A. M. Rey for discussions concerning the realization and observation of topological insulators. A.M.E. thanks R. S. K. Mong and J. E. Moore for earlier collaboration on AFTIs. A.M.E. was supported by DOE Award No. DE-SC0003910 and V.G. by NSF Grants No. PHY-0904017 and No. PHY-0551164. V.G. is also grateful to The Kavli Institute for Theoretical Physics, Santa Barbara and the Physics Department of the University of Melbourne where part of this work was done.

- ¹C. Nayak, S. H. Simon, A. Stern, M. Freedman, and S. Das Sarma, *Rev. Mod. Phys.* **80**, 1083 (2008).
- ²M. Z. Hasan and C. L. Kane, *Rev. Mod. Phys.* **82**, 3045 (2010).
- ³X.-L. Qi, T. L. Hughes, and S.-C. Zhang, *Phys. Rev. B* **78**, 195424 (2008).
- ⁴S. Ryu, A. P. Schnyder, A. Furusaki, and A. W. W. Ludwig, *New J. of Phys.* **12**, 065010 (2010).
- ⁵M. Levin and A. Stern, *Phys. Rev. Lett.* **103**, 196803 (2009); J. Maciejko, X.-L. Qi, A. Karch, and S.-C. Zhang, *ibid.* **105**, 246809 (2010); B. Swingle, M. Barkeshli, J. McGreevy, and T. Senthil, *Phys. Rev. B* **83**, 195139 (2011).
- ⁶L. Fu, C. L. Kane, and E. J. Mele, *Phys. Rev. Lett.* **98**, 106803 (2007).
- ⁷J. E. Moore and L. Balents, *Phys. Rev. B* **75**, 121306 (2007).
- ⁸R. Roy, *Phys. Rev. B* **79**, 195322 (2009).
- ⁹Y.-J. Lin, R. L. Compton, K. Kimenez-Garcia, J. V. Porto, and I. B. Spielman, *Nature (London)* **462**, 628 (2009).
- ¹⁰N. Goldman, I. Satija, P. Nikolic, A. Bermudez, M. A. Martin-Delgado, M. Lewenstein, and I. B. Spielman, *Phys. Rev. Lett.* **105**, 255302 (2010).
- ¹¹B. Béri and N. R. Cooper, *Phys. Rev. Lett.* **107**, 145301 (2011).
- ¹²P. Hosur, S. Ryu, and A. Vishwanath, *Phys. Rev. B* **81**, 045120 (2010).
- ¹³R. S. K. Mong, A. M. Essin, and J. E. Moore, *Phys. Rev. B* **81**, 245209 (2010).
- ¹⁴A. M. Essin, J. E. Moore, and D. Vanderbilt, *Phys. Rev. Lett.* **102**, 146805 (2009).
- ¹⁵A. M. Turner, Y. Zhang, R. S. K. Mong, and A. Vishwanath, e-print [arXiv:1010.4335](https://arxiv.org/abs/1010.4335).
- ¹⁶L. Fu and C. L. Kane, *Phys. Rev. B* **76**, 045302 (2007); T. L. Hughes, E. Prodan, and B. A. Bernevig, *ibid.* **83**, 245132 (2011).
- ¹⁷A. Altland and M. R. Zirnbauer, *Phys. Rev. B* **55**, 1142 (1997); M. Zirnbauer, *J. Math. Phys.* **37**, 4986 (1996); A. Kitaev, *AIP Conf. Proc.* **1134**, 22 (2009).
- ¹⁸A. P. Schnyder, S. Ryu, A. Furusaki, and A. W. W. Ludwig, *Phys. Rev. B* **78**, 195125 (2008).
- ¹⁹M. Silaev and G. Volovik, *J. Low Temp. Phys.* **161**, 460 (2010).
- ²⁰A. M. Essin and V. Gurarie, *Phys. Rev. B* **84**, 125132 (2011).
- ²¹V. Gurarie and L. Radzihovsky, *Phys. Rev. B* **75**, 212509 (2007).
- ²²E. H. Lieb, *Phys. Rev. Lett.* **62**, 1201 (1989).
- ²³Note that this disconnected band violates the usual bulk-boundary correspondence for a TI.^{4,20} Our model also has nontrivial 1D chiral invariants for each lattice direction, which are responsible for this violation, as they require disconnected bands.
- ²⁴E. Tang, J.-W. Mei, and X.-G. Wen, *Phys. Rev. Lett.* **106**, 236802 (2011); K. Sun, Z. Gu, H. Katsura, and S. Das Sarma, *ibid.* **106**, 236803 (2011); X. Hu, M. Kargarian, and G. A. Fiete, *Phys. Rev. B* **84**, 155116 (2011).
- ²⁵D. Jaksch and P. Zoller, *New J. Phys.* **5**, 56 (2003); F. Gerbier and J. Dalibard, *ibid.* **12**, 033007 (2010).
- ²⁶M. Bishof, M. J. Martin, M. D. Swallows, C. Benko, Y. Lin, G. Quéméner, A. M. Rey, and J. Ye, *Phys. Rev. A* **84**, 052716 (2011).
- ²⁷J. T. Stewart, J. P. Gaebler, and D. S. Jin, *Nature (London)* **454**, 744 (2008).
- ²⁸The solid-state literature that derives this result^{3,14,38} considers charged particles, and in a neutral system one needs to divide the constant e^2/h by $e\gamma$, with e the charge and $\gamma = e/2m$ the classical gyromagnetic ratio.
- ²⁹V. Schweikhard, I. Coddington, P. Engels, V. P. Mogendorff, and E. A. Cornell, *Phys. Rev. Lett.* **92**, 040404 (2004).
- ³⁰N. Gemelke, E. Sarajlic, and S. Chu, e-print [arXiv:1007.2677](https://arxiv.org/abs/1007.2677).
- ³¹D. Ceresoli, T. Thonhauser, D. Vanderbilt, and R. Resta, *Phys. Rev. B* **74**, 024408 (2006); T. Thonhauser, D. Ceresoli, D. Vanderbilt, and R. Resta, *Phys. Rev. Lett.* **95**, 137205 (2005); J. Shi, G. Vignale, D. Xiao, and Q. Niu, *ibid.* **99**, 197202 (2007); D. Xiao, J. Shi, and Q. Niu, *ibid.* **95**, 137204 (2005); M. G. Lopez, D. Vanderbilt, T. Thonhauser, and I. Souza, *Phys. Rev. B* **85**, 014435 (2012); T. Thonhauser, *Int. J. Mod. Phys. B* **25**, 1429 (2011).
- ³²F. Chevy, K. W. Madison, and J. Dalibard, *Phys. Rev. Lett.* **85**, 2223 (2000); P. C. Haljan, B. P. Anderson, I. Coddington, and E. A. Cornell, *ibid.* **86**, 2922 (2001).
- ³³J. Stenger, S. Inouye, A. P. Chikkatur, D. M. Stamper-Kurn, D. E. Pritchard, and W. Ketterle, *Phys. Rev. Lett.* **82**, 4569 (1999).
- ³⁴V. Gurarie, *Phys. Rev. B* **83**, 085426 (2011).
- ³⁵D. Pesin and L. Balents, *Nature Phys.* **6**, 376 (2010).
- ³⁶J. Ye, Y. B. Kim, A. J. Millis, B. I. Shraiman, P. Majumdar, and Z. Tešanović, *Phys. Rev. Lett.* **83**, 3737 (1999).
- ³⁷B. Binz, A. Vishwanath, and V. Aji, *Phys. Rev. Lett.* **96**, 207202 (2006).
- ³⁸A. Malashevich, I. Souza, S. Coh, and D. Vanderbilt, *New J. Phys.* **12**, 053032 (2010).